Title

Independent amplitude approximations in coupled cluster valence bond theory: Incorporation of 3-electron-pair correlation and application to spin frustration in the low-lying excited states of a ferredoxin-type tetrametallic iron-sulfur cluster

Journal

The Journal of Chemical Physics, 149(14)

ISSN

0021-9606

Authors

Small, David W

Head-Gordon, Martin

Publication Date

2018-10-14

DOI

10.1063/1.5046318

Peer reviewed

Independent amplitude approximations in coupled cluster valence bond theory: Incorporation of 3-electron-pair correlation and application to spin frustration in the low-lying excited states of a ferredoxin-type tetrametallic iron-sulfur cluster

David W. Small and Martin Head-Gordon

Department of Chemistry, University of California, Berkeley, California 94720, USA and Chemical Sciences Division, Lawrence Berkeley National Laboratory, Berkeley, California 94720, USA

(Dated: September 16, 2018)

Abstract

Coupled cluster valence bond (CCVB) is a simple electronic structure method based on a perfect pairing (PP) reference with 2-pair recouplings for strong electron correlation problems. CCVB is spin-pure, size-consistent, and can exactly (in its active space) separate any molecule into atoms for which unrestricted Hartree-Fock at dissociation is the sum of the ground state UHF energies. However CCVB is far from a complete description of strong correlations. Its first failure to exactly describe spin-recouplings arises at the level of 3 electron pairs, such as the recoupling of 3 triplet oxygen atoms in the dissociation of singlet ozone. Such situations are often associated with spin frustration. To address this limitation, an extension of CCVB, termed CCVB+i3, is reported here that includes an independent (i) amplitude approximation to the 3-pair recouplings. CCVB+i3 thereby has the same basic computational requirements as those of CCVB, which has previously been shown to be an efficient method. CCVB+i3 correctly separates molecules that CCVB cannot. As a by-product, an independent 2-pair amplitude approximation to CCVB, called PP+i2, is also defined. Remarkably, PP+i2 can also correctly separate systems that CCVB cannot. CCVB+i3 is validated on the symmetric dissociation of D_{3h} ozone. CCVB+i3 is then used to explore the role of 3-pair recouplings in an $[Fe_4S_4(SCH_3)_4]^{2-}$ cluster that has been used to model the iron-sulfur core of $[Fe_4S_4]$ ferredoxins. Using localized PP orbitals, such recouplings are demonstrated to be large in some low-lying singlet excited states of the cluster. Significant 3 pair recoupling amplitudes include the usual triangular motif associated with spin frustration, and other geometric arrangements of the 3 entangled pairs across the 4 iron centers.

I. INTRODUCTION

Most practical electronic structure calculations are performed using density functional theory (DFT) methods[1,2], because the accuracy of standard functionals[3,4] is adequate for chemical applications to many complex systems, such as catalytic processes[5]. Furthermore there have been continued improvements in the accuracy of new functionals[3,4,6,7]. However, DFT has well-documented limitations[8], such as the delocalization and strong correlation errors, which affect a range of significant problems, such as relative energies of different spin states in transition metal-containing systems[9,10]. For much greater computational cost, standard wavefunction methods[11,12] based on a single determinant Hartree-Fock (HF) reference, such as coupled cluster theory with single and double substitutions, corrected for triple substitutions via CCSD(T)[13], are able to exceed the accuracy of DFT, and do not suffer from the delocalization error.

However, addressing the strong correlation (SC) problem lies beyond approaches such as standard DFT or single-reference wavefunction methods. By contrast, SC is defined by large numbers of electron configurations making essential contributions to the wavefunction. Methods to address SC are diverse, and we can only briefly mention a few main directions here. SC models begin with brute force solution of the Schrodinger equation in a subspace of essential orbitals via complete active space (CAS) methods[14–16] or related approaches based on spin-flipping[17,18]. Recently there have been promising efforts to more efficiently solve that problem, by selecting essential configurations either stochastically[19] or deterministically[20,21] with both approaches yielding much softer exponential scaling. Lower scaling approaches are possible based on reduced density matrices[22,23], or the density matrix renormalization group[24,25]. One can also approximate the CAS wavefunction, for example by special types (restricted or generalized active spaces) of configuration selection[26–28] or coupled cluster theory[29–32]. Nonetheless, the SC problem remains open because at present only the exponentially scaling brute force methods can guarantee satisfactory accuracy in all types of SC cases.

This work is concerned with extending the domain of applicability of the coupled cluster (CC) valence bond (VB) approach[33–36] to SC. CCVB is an example of a physically motivated ansatz for SC, which approximates spin-coupled valence bond theory[37–39] at dramatically lower computational cost. CCVB can also be viewed as a generalization of spin projected

unrestricted HF (PUHF)[40] with improved physical properties. Like PUHF, CCVB has correct spin symmetry, is suitable for small strongly correlated systems, and is (empirically) variational. Unlike PUHF, CCVB is size consistent and is thereby potentially suitable for large strongly correlated systems. CCVB has been extended to open shell systems, with very encouraging results[36]. The fundamental ideas of CCVB have also been used to create a generalization of CCSD for even electron systems, termed CCVB-SD[41,42], that treats SC far better than CCSD itself (though at much greater cost than CCVB).

Concentrating on singlet spin states, the CCVB wave function[33,34] has the form of an unconventional CC expansion that begins with the Perfect Pairing (PP) wave function[43,44], which is an antisymmetrized product of simple singlet pair wave functions. Generally, the PP pairs may be identified as one of core electrons, bonds, or lone pairs. Each pair is the solution of a 2 electron in 2 orbital problem, and thus pairs associated with single bonds can dissociate correctly. CCVB traverses a hierarchy of configurations that substitute the singlet pairs with triplet pairs, where the independent variables are 2-pair recoupling amplitudes. The substituted configurations provide the leading contribution to the correlation between the bonding pairs. Despite its simplicity, CCVB has a remarkable exactness property. Reflecting its link to PUHF, it can separate a closed shell molecule into separated atoms for any system where at dissociation the UHF energy equals the sum of the ground-state UHF energies of the atoms[33,34].

CCVB is far from a complete treatment of active space correlations. One fundamental omission is that closed shell CCVB has no contribution from 3-pair substituted configurations (nor with those involving any odd number of pairs). This is because the PUHF wave function does not overlap with these configurations. The first purpose of this paper is obtain a working approach to inclusion of these configurations, as an extension to CCVB. The resulting theory is presented in Section II, leading to tractable working equations that can be implemented within electronic structure software packages. The 3-pair recouplings are treated via an independent amplitude approximation so that they can be solved without iterations, while directly influencing the (iterative) CCVB equations for the 2-pair recouplings in a self-consistent manner. Reflecting this hybrid nature, the method is called CCVB+i3.

The second purpose of this work is to begin to explore situations in which the 3-pair recouplings make a significant contribution to electron correlations. The 3-pair and associated configurations are an essential part of the configuration space, and thereby they

significantly contribute to numerous states, although these are not necessarily energetically low-lying in many systems. We can get an introductory idea of when 3-pair correlations are important (to low-lying states) by considering the dissociation of singlet states of small molecules into high spin fragments. To do this, we distinguish two classes: states for which the corresponding $s_z = 0$ UHF solution dissociates correctly, i.e. the UHF energy is the sum of the energies for the pertinent fragments, and those for which this is not true. The former class contains systems like N_2 and square-planar Cr_4, and, reflecting the exactness property already mentioned, every example in this class can be dissociated correctly by CCVB. In this class, there should typically be no major 3-pair correlations in low-lying states.

The latter class contains systems like CO_2 and pentagonal Cr_5, and its members, in general, cannot be dissociated correctly by CCVB. These systems are typically spin frustrated in the stretched-bond region of the potential energy surface (PES). They have triads of interacting bonds associated with 3 or more atoms in arrangements typical of spin frustration, such as triangles. Such triads exhibit large 3-pair correlations, and they do not occur in systems in the former class. These concepts will become more concrete with the examples presented in Section III below. We first consider the lowest singlet state of triangular O_3, which provides an elementary example of 3 bonds in a spin-frustrated-type arrangement. After that, we consider a much more complicated [4Fe-4S] iron-sulfur cubane complex, $[Fe_4S_4(SCH_3)_4]^{2-}$, similar to those found in ferredoxin cores. This complex has previously been used as a model system in a pioneering study[45] that explored the dense, low-lying energy spectrum using the DMRG method. Applying the CCVB+i3 approach establishes that this complex has extensive 3-pair correlation in its low-lying singlet states (though not the ground state), and this provides significant insight into the nature of the bond triads producing this correlation.

II. THEORY

In this paper, we will restrict the development to singlet systems. Open-shell systems involve some additional theory that will be treated separately in a forthcoming paper.[46] We will now briefly describe some CCVB prerequisites.

The CCVB wave function uses a PP reference wave function. The latter is an antisymmetrized product of $n_p \equiv \frac{n_e}{2}$ geminals, with n_e being the total number of electrons. Some

of these geminals may be "inactive", i.e. they are basically a doubly occupied orbital. The remaining geminals are active, and each of these is a two electrons in two orbitals, i.e. (2,2), wave function. All of the mentioned orbitals are orthogonal, and hence the geminals are "strongly orthogonal".

More explicitly, the PP wave function may be written as

$$|\Psi_0\rangle = \left(\prod_{k=1}^{n_p} \mathbf{g}^\dagger_{\mathbf{s},k}\right)|0\rangle. \tag{1}$$

This expression uses second quantization and consists of creation operators for the n_p pairs acting on the vacuum state. These pair creation operators are defined by

$$\mathbf{g}^\dagger_{\mathbf{s},k} = \frac{1}{\sqrt{2(1+\cos^2(\theta_k))}}\left(2\cos(\theta_k)\,\mathbf{a}^\dagger_{k_\alpha}\mathbf{a}^\dagger_{k_\beta} - \sin(\theta_k)\,\mathbf{a}^\dagger_{k_\alpha}\mathbf{a}^\dagger_{\hat{k}_\beta} - \sin(\theta_k)\,\mathbf{a}^\dagger_{\hat{k}_\alpha}\mathbf{a}^\dagger_{k_\beta}\right). \tag{2}$$

The single-electron creation operators correspond to the orbitals mentioned above, with k and $\hat{k}$ indexing a particular choice of two orbitals spanning the (2,2) active space, α and β are the usual spin labels, and the θ_k are "polarization" angles: $\theta_k = 0$ corresponds to an uncorrelated pair, while $\theta_k = \frac{\pi}{2}$ corresponds to a biradical pair.

Many other configurations contribute to the CCVB wave function. Each of these is obtained by substituting a subset of the singlet geminals with triplet geminals in a manner that gives an overall singlet. The triplet geminals may be defined by

$$\begin{aligned}
\mathbf{g}^\dagger_{\mathbf{t_1},k} &= \frac{1}{\sqrt{2}}(-\mathbf{a}^\dagger_{k_\alpha}\mathbf{a}^\dagger_{\hat{k}_\beta} + \mathbf{a}^\dagger_{\hat{k}_\alpha}\mathbf{a}^\dagger_{k_\beta}) \\
\mathbf{g}^\dagger_{\mathbf{t_2},k} &= \mathbf{a}^\dagger_{k_\alpha}\mathbf{a}^\dagger_{\hat{k}_\alpha} \\
\mathbf{g}^\dagger_{\mathbf{t_3},k} &= \mathbf{a}^\dagger_{k_\beta}\mathbf{a}^\dagger_{\hat{k}_\beta}.
\end{aligned} \tag{3}$$

Similar to conventional CC, these substitutions are grouped as "doubles", "triples", "quadruples", etc. The doubly substituted configurations, denoted by $|\Psi_{(kl)}\rangle$ are obtained by the following replacement in eq. (1)

$$\mathbf{g}^\dagger_{\mathbf{s},k}\mathbf{g}^\dagger_{\mathbf{s},l} \;\rightarrow\; \mathbf{d}^\dagger_{\mathbf{s_2},kl} = \frac{1}{\sqrt{3}}\big(\mathbf{g}^\dagger_{\mathbf{t_1},k}\mathbf{g}^\dagger_{\mathbf{t_1},l} - \mathbf{g}^\dagger_{\mathbf{t_2},k}\mathbf{g}^\dagger_{\mathbf{t_3},l} - \mathbf{g}^\dagger_{\mathbf{t_3},k}\mathbf{g}^\dagger_{\mathbf{t_2},l}\big). \tag{4}$$

The triply substituted configurations, denoted by $|\Psi_{(klm)}\rangle$, are obtained by the following replacement in eq. (1)

$$\mathbf{g}^\dagger_{\mathbf{s},k}\mathbf{g}^\dagger_{\mathbf{s},l}\mathbf{g}^\dagger_{\mathbf{s},m} \;\rightarrow\; \mathbf{e}^\dagger_{\mathbf{s_5},klm}, \tag{5}$$

where

$$\mathbf{e}^{\dagger}_{\mathbf{s_5},klm} = \frac{1}{\sqrt{6}}\Big(\mathbf{g}^{\dagger}_{\mathbf{t_1},k}(\mathbf{g}^{\dagger}_{\mathbf{t_2},l}\mathbf{g}^{\dagger}_{\mathbf{t_3},m} - \mathbf{g}^{\dagger}_{\mathbf{t_3},l}\mathbf{g}^{\dagger}_{\mathbf{t_2},m}) - \mathbf{g}^{\dagger}_{\mathbf{t_2},k}\mathbf{g}^{\dagger}_{\mathbf{t_1},l}\mathbf{g}^{\dagger}_{\mathbf{t_3},m} + \mathbf{g}^{\dagger}_{\mathbf{t_3},k}\mathbf{g}^{\dagger}_{\mathbf{t_1},l}\mathbf{g}^{\dagger}_{\mathbf{t_2},m} + (\mathbf{g}^{\dagger}_{\mathbf{t_2},k}\mathbf{g}^{\dagger}_{\mathbf{t_3},l} - \mathbf{g}^{\dagger}_{\mathbf{t_3},k}\mathbf{g}^{\dagger}_{\mathbf{t_2},l})\mathbf{g}^{\dagger}_{\mathbf{t_1},m}\Big). \tag{6}$$

One way of viewing a 3-pair substitution is as a coupling of two triplet pairs to a triplet, which is then coupled to the remaining triplet pair to get an overall singlet. In this way, 3-pair correlation is rather different from 2-pair correlation, and this is consistent with the geometric distinctions between systems that do and do not exhibit large 3-pair amplitudes.

All of the remaining configurations are obtained by making multiple applications of the above replacements. Each of these configurations is labelled by the indices of the substituted pairs, with parentheses around those for each double or triple sub-substitution.

The CCVB wave function $|\Psi\rangle$, normalized as $\langle\Psi_0|\Psi\rangle = 1$, is fully defined by the following. The 2-pair amplitudes are variables to be computed

$$t_{kl} = \langle\Psi_{(kl)}|\Psi\rangle. \tag{7}$$

The 3-pair amplitudes are 0:

$$\langle\Psi_{(klm)}|\Psi\rangle = 0. \tag{8}$$

The same is true of all other substitutions of an odd number of pairs. The CCVB wave function has a CC property

$$\langle\Psi_{(kl)(mn)}|\Psi\rangle = t_{kl}t_{mn}, \tag{9}$$

$$\langle\Psi_{(kl)(mn)(op)}|\Psi\rangle = t_{kl}t_{mn}t_{op}, \tag{10}$$

etc. In this way even-electron excitations are constructed as products of the variables describing the doubles, which recouple 2 triplet pairs to a singlet.

The 2-pair amplitudes, which we group into a vector $\mathbf{t}$, are computed by solving the set of equations $\mathrm{R}_{kl}(\mathbf{t}) = 0$, where

$$\mathrm{R}_{kl}(\mathbf{t}) = \langle\Psi_{(kl)}|\mathbf{H}|\Psi\rangle - t_{kl}E, \tag{11}$$

where $\mathbf{H}$ is the Hamiltonian operator and

$$E = \langle\Psi_0|\mathbf{H}|\Psi\rangle \tag{12}$$

is the energy. Note that for two configurations to interact through $\mathbf{H}$, their respective total spins for each pair, i.e. singlet or triplet, can differ only for 2 pairs or less. This is similar to the Slater-Condon rules for determinants. Thus, $|\Psi_0\rangle$ only interacts through $\mathbf{H}$ with itself and the doubly-substituted configurations, and $|\Psi_{(kl)}\rangle$ interacts only with the reference configuration and (selected members of) the doubly, triply, and quadruply-substituted configurations. The CCVB equations can thereby be brought into the following simple form

$$\mathrm{R}_{kl}(\mathbf{t}) = \mu_{kl}(1 - t_{kl}^2) + t_{kl}\omega_{kl} + \sum_{m \notin \{k,l\}} \Big[t_{km}(\kappa_{lm} - t_{kl}\mu_{km}) + t_{lm}(\kappa_{km} - t_{kl}\mu_{lm}) \Big], \tag{13}$$

where

$$\kappa_{km} = \langle \Psi_{(kl)} | \mathbf{H} | \Psi_{(lm)} \rangle, \tag{14}$$

$$\mu_{kl} = \langle \Psi_0 | \mathbf{H} | \Psi_{(kl)} \rangle, \tag{15}$$

and

$$\omega_{kl} = \langle \Psi_{(kl)} | \mathbf{H} | \Psi_{(kl)} \rangle - \langle \Psi_0 | \mathbf{H} | \Psi_0 \rangle. \tag{16}$$

This process may be viewed as solving the eigenvalue problem within the doubles subspace. It, together with orbital optimization of the energy, defines the CCVB model. We have now given enough basic CCVB information to start discussing the incorporation of 3-pair correlation.

A. CCVB with 3-pair correlations: Independent Amplitude Approximation

In a general CC manner, the triples amplitudes can be introduced and combined with each other to make a contribution to the coefficients for the 6-pair-substituted configurations, or combined with the doubles to give non-zero coefficients on the 5-pair-substituted configurations, and so on for higher order substitutions. That is, introducing non-zero triples will not (directly) affect the coefficients for the quadruply-substituted configurations. Doubly and triply substituted configurations must share two indices if they are to interact through $\mathbf{H}$. The doubles amplitude residual for a generic 3-pair model is therefore simply

$${}^{3\mathrm{p}}\mathrm{R}_{kl}(\mathbf{t}) = \mathrm{R}_{kl}(\mathbf{t}) + \sum_{m \notin \{k,l\}} \kappa_{kl;m} t_{klm}, \tag{17}$$

where

$$\kappa_{kl;m} = \langle \Psi_{(kl)} | \mathbf{H} | \Psi_{(klm)} \rangle. \tag{18}$$

Note that $|\Psi_{(klm)}\rangle$ is antisymmetric under permutations of the 3 indices, and this configuration appears with different index orderings in the above equations.

The immediate inclination for how to compute the triples amplitudes is perhaps to assume an overall CCVB wave function with CC structure akin to eqns. (9) and (10), e.g.

$$\langle \Psi_{(kl)(mno)} | \Psi \rangle \stackrel{?}{=} t_{kl} t_{mno}, \tag{19}$$

and so on for higher order terms. The trouble with this is that, for a selection of 5 pairs, there are 10 associated pentuply substituted configurations, yet they span only a 6-dimensional subspace. That is, the configurations are linearly dependent. Thus, there may not always exist a CCVB wave function that obeys eq. (19) (for each choice of indices). Such a wave function will exist in the dissociation limit, but this wave function form may pose problems with size consistency more generally. We will discuss this further in a subsequent paper.[46]

1. *Independent Amplitude Approximation: doubles*

It turns out that one way to obtain a working CCVB model that includes 3-pair couplings is to use an independent amplitude approximation (IAA). This derives from a simple observation: for familiar bond dissociations like that of N_2, the "off-diagonal" terms of eq. (13), i.e. the terms in $\mathrm{R}_{kl}(\mathbf{t})$ involving t_{km} or t_{lm}, cancel in the dissociation limit. Therefore, if we switch to using

$$^{(2)}\mathrm{R}_{kl}(\mathbf{t}) = \mu_{kl}(1 - t_{kl}^2) + t_{kl}\omega_{kl} \tag{20}$$

for the amplitude-equation residuals, then the correct amplitudes and energy, i.e. the same as those of regular CCVB, will be reached in the dissociation limit for these cases. We will call this model "PP+i2", because its 2-pair amplitudes are treated independently (i), i.e. we are solving a local eigenvalue problem for each 2-pair selection:

$$^{(2)}\mathrm{R}_{kl}(\mathbf{t}) = \langle \Psi_{(kl)} | \mathbf{H} | \Xi_{(kl)} \rangle - t_{kl}\big(\langle \Psi_0 | \mathbf{H} | \Xi_{(kl)} \rangle\big), \tag{21}$$

where

$$|\Xi_{(kl)}\rangle = |\Psi_0\rangle + t_{kl}|\Psi_{(kl)}\rangle. \tag{22}$$

This is similar in spirit to the Independent Electron Pair Approximation (IEPA)[47–49] of conventional CC theory. This supplements the PP treatment of correlation within each electron pair.

PP+i2 therefore shares some nice properties with CCVB: correct spin symmetry, correct dissociation for a wide class of molecules (although see the discussion below on long-range strong correlation for some subtle exceptions to this), and it is size consistent. For singlet systems in the CCVB context, size consistency means that all interfragment doubles (and triples, if present) go to 0 in the limit of dissociating the molecule into singlet fragments. It is readily clear that PP+i2 satisfies this property.

Remarkably, we have observed that PP+i2 correctly dissociates the molecules that CCVB cannot, i.e. the ones that, within a more complete model, would exhibit large 3-pair correlation. Thus, given CCVB's incorrectness in these situations, the off-diagonal terms in eq. (13) do not cancel in the dissociation limit, but, we infer, they do get cancelled by the extra terms included in eq. (17), assuming the correct triples amplitudes are included.

PP+i2 handles the dissociation limit, but what about other parts of the PES? We have observed that PP+i2 often performs surprisingly well in the equilibrium and intermediate-bond-breaking PES regions; evidence for this will be shown below and in the second paper.[46] This is in contrast to IEPA, which is typically significantly non-variational in these regions.

Understandably, this very simple model does have some limitations. It is possible for the energy of a doubly substituted configuration to drop significantly below that of the reference, and in this case the pertinent PP+i2 amplitude will be very large. Thus, the PP+i2 amplitudes sometimes "blow up" during the orbital optimization, causing significantly non-variational energies. CCVB, according to our long experience with the model, is highly immune to such behavior. Indeed, we have repeatedly observed that halting an erratic PP+i2 calculation and recomputing the amplitudes with CCVB produces unremarkable amplitudes and a high energy. In other words, the orbitals are far from the optimal CCVB ones in this situation. In fact, one way to resolve this PP+i2 issue is to begin the calculation with CCVB optimized orbitals.

To reveal another problem with PP+i2, consider situations in which $\mu_{kl} = 0$ in eq. (20). These matrix elements vanish whenever the associated pairs are well separated, and $t_{kl} = 0$ is the invariably the result in PP+i2. This behavior is correct for simple situations such as the separation of two N_2 molecules with the k and l pairs localized to separate molecules.

But, as we have recently shown,[36] there are other cases in which there are well-separated pairs associated with large doubles amplitudes. Systems exhibiting this very long-range strong correlation cannot properly be described with PP+i2.

2. Independent Amplitude Approximation: triples

Despite the above limitations, the successes of PP+i2 are noteworthy. This makes it intrinsically useful, and perhaps more importantly, it validates the independent amplitude approximation concept. This motivates a similar approximation for the 3-pair amplitudes, as an extension of CCVB. One way of viewing the PP+i2 amplitude equations is that each $|\Psi_{(kl)}\rangle$ interacts only with the other configurations whose substitution indices form a subset of $\{k, l\}$, i.e. only itself and the reference. Applying this idea to the 3-pair situation, we allow $|\Psi_{(klm)}\rangle$ to interact only with $|\Psi_0\rangle$, $|\Psi_{(kl)}\rangle$, $|\Psi_{(km)}\rangle$, and $|\Psi_{(lm)}\rangle$. We get the following residual for the 3-pair amplitudes:

$$^{(3)}\mathrm{R}_{klm}(\mathbf{t}) = \langle\Psi_{(klm)}|\mathbf{H}|\Xi_{(klm)}\rangle - t_{klm}\big(\langle\Psi_0|\mathbf{H}|\Xi_{(klm)}\rangle\big), \tag{23}$$

where the local wave function for a selected 3-pair substitution is

$$|\Xi_{(klm)}\rangle = |\Psi_0\rangle + t_{kl}|\Psi_{(kl)}\rangle + t_{km}|\Psi_{(km)}\rangle + t_{lm}|\Psi_{(lm)}\rangle + t_{klm}|\Psi_{(klm)}\rangle. \tag{24}$$

The 3-pair amplitudes are then given simply by

$$t_{klm} = -\frac{\kappa_{kl;m}t_{kl} - \kappa_{km;l}t_{km} + \kappa_{lm;k}t_{lm}}{\omega_{klm} - \mu_{kl}t_{kl} - \mu_{km}t_{km} - \mu_{lm}t_{lm}}, \tag{25}$$

where

$$\omega_{klm} = \langle\Psi_{(klm)}|\mathbf{H}|\Psi_{(klm)}\rangle - \langle\Psi_0|\mathbf{H}|\Psi_0\rangle. \tag{26}$$

These equations, along with eq. (17), define a 3-pair model that we will call CCVB+i3. Because the triples equations are so simple, we can think of CCVB+i3 as a modified CCVB doubles model, and indeed its scaling with system size is the same as that of CCVB. This stems from the fact that the new matrix elements found in eq. (25) are efficient to compute. The practical computation of the $\kappa_{kl;m}$ is discussed in ref. 36, and the ω_{klm} can be computed in cubic time, as will be described in the second paper.[46] There, we will also discuss the orbital optimization component of CCVB+i3, noting for now that the process is very similar

to that of CCVB. We may therefore conclude that CCVB+i3 has essentially the same computational requirements as CCVB. In our current implementation, CCVB is rate-limited by a fifth-order scaling integral transformation that becomes quartic for large molecules.[35] We have previously demonstrated that CCVB calculations with active spaces of 228 correlated electrons are feasible on a single processor.[35]

Following the discourse used above for PP+i2, it is straightforward to show that CCVB+i3 is size consistent. It is evident that it can dissociate any state correctly. The fact that it includes the full structure of CCVB leads us to anticipate that it will significantly improve or eliminate the main problems with PP+i2, particularly non-variational blow ups and issues for systems with very long-range strong correlation. We are now ready to consider example calculations with these models.

III. CALCULATIONS

Two methods were described in Section II. The main result is the CCVB+i3 model which extends CCVB theory by use of an independent amplitude approximation (IAA) for 3-pair recouplings (IAA-3). As a by-product a very simple extension to perfect pairing which includes IAA-2 amplitudes was obtained, termed PP+i2. PP+i2 is an approximation to CCVB (though as discussed above, it also has the striking property of being able to dissociate systems correctly that CCVB cannot). Thus a well-defined hierarchy of post-PP methods is PP+i2, CCVB, CCVB+i3. The implementation of CCVB previously reported[35] in the Q-Chem program[50] has been extended to include PP+i2 and CCVB+i3, and was used for all the examples described below. Q-Chem was also used for all HF calculations, and CASSCF calculations used the GAMESS program.[51]

A. Triangular O_3

We begin with a simple illustrative example: the symmetric dissociation of triangular (D_{3h}) O_3 in its singlet state. In the dissociation limit, the singlet ground state for this system is a coupling of 3 triplet O atoms. UHF can assign only $s_z = 1$ or $s_z = -1$ to a triplet O atom, so only the overall $s_z = 1$ and $s_z = 3$ UHF curves will reach the correct dissociation limit. Similarly, we expect that CCVB will be unable to correctly dissociate the

singlet state. We plot the energy curves for PP+i2, CCVB, CCVB+i3, UHF, generalized HF (GHF), and CASSCF in Fig. 1. The cc-pVTZ basis[52] was used for all these calculations. We used 3 active pairs for the CCVB-type methods, and the corresponding (6,6) active space for CASSCF; because each triplet O atom has two unpaired electrons, this is the smallest active space that can provide a qualitatively correct PES for this system.

Indeed, the CCVB energy is too high at dissociation, as opposed to conventional restricted CC energies which are typically too low in bond breaking situations. At dissociation, the CCVB spin coupling of the 6 active electrons is not equal to the singlet coupling of 3 triplets (although it is not orthogonal to the latter), and therefore the CCVB spin coupling includes components involving (1 or 3) singlet oxygen atoms. This is consistent with the high energy

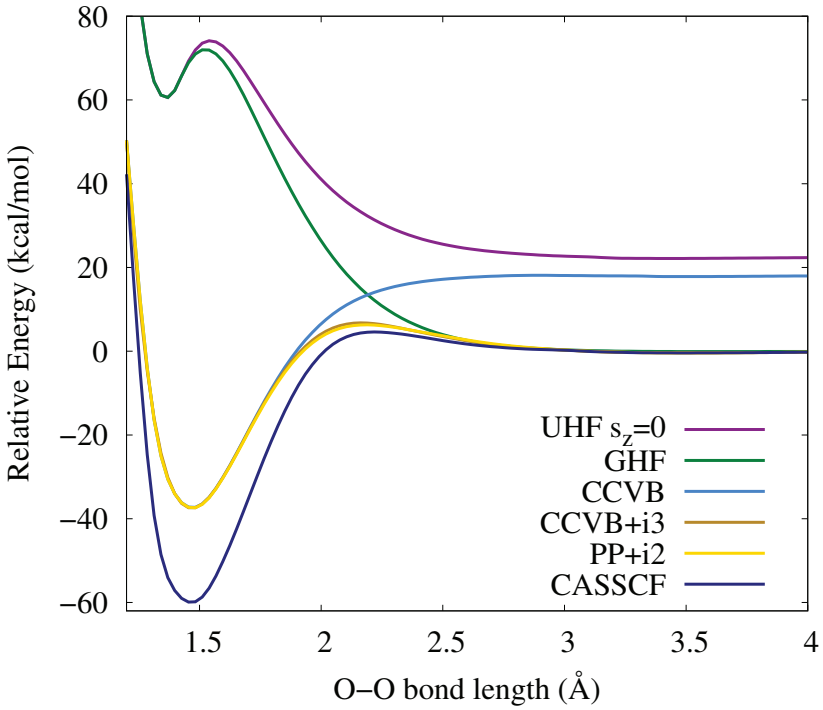

FIG. 1: Potential energy curves for the symmetric dissociation (D_{3h}) of singlet O_3 to three triplet O atoms. Results in the cc-pVTZ basis are shown for Hartree-Fock methods (UHF, GHF), coupled cluster valence bond methods (PP+i2, CCVB, CCVB+i3) using 3 active pairs, and (6,6) CASSCF, which provides the exact result in that active space. It is evident that UHF and CCVB fail to reach the correct dissociation limit, while GHF, PP+i2, and CCVB+i3 dissociate correctly.

at dissociation.

By contrast, PP+i2 and CCVB+i3 are both correct at dissociation and their energy curves are very similar across the whole PES. This degree of similarity is higher than what is typical, as will be shown below in a different system. But this example confirms that PP+i2 retains the desirable molecular dissociation property of CCVB and extends this to any dissociation situation. The PP+i2, CCVB, and CCVB+i3 equilibrium geometries are all accurate relative to CASSCF, while the bond length in UHF and GHF is too short. The binding energies of PP+i2, CCVB, and CCVB+i3 are reasonably accurate relative to CASSCF, while UHF and GHF are highly inaccurate here, predicting a significantly unbound molecule.

UHF and GHF split early in the dissociation, and because of their short equilibrium bond length, this is even before CASSCF reaches its equilibrium bond length. The UHF solution is internally (UHF $\rightarrow$ UHF) stable at all geometries. Using our spin collinearity test[53], the GHF solution was confirmed to be noncollinear for all points to the right of about 1.41 Å. The testing also revealed that this GHF wave function has $\langle \mathbf{S}_x \rangle = \langle \mathbf{S}_y \rangle = \langle \mathbf{S}_z \rangle = 0$ for every geometry. That is, the expectation values for the three axial spin operators are always zero for this solution. Thus, this solution, although significantly spin contaminated, may be said to be of the "singlet type", in a sense similar to how this phrase is applied to UHF in the dissociation of N_2. It is notable that such a GHF solution reaches the correct dissociation limit. This is in contrast to the symmetric dissociation of CO_2. In that case, the end result is also 3 triplet atoms, but in a previous paper[53], were unable to find a GHF solution that dissociates correctly and has vanishing spin expectation values.

We also note that for O_3, the above GHF solution is not the lowest for all stretched geometries. A collinear solution for $s_z = 1$ drops below it near 2 Å, and later on a collinear $s_z = 3$ solution becomes the lowest. These latter solutions have only slightly lower energies than those of the above GHF solution, with a maximum difference of around 1 kcal/mol. The above GHF solution remains stable until around 2.4 Å.

B. Iron-Sulfur Cluster

In this subsection, we perform calculations on a $[Fe_4S_4(SCH_3)_4]^{2-}$ cluster. In a recent article,[45] this cluster was used to model the iron-sulfur core of $[Fe_4S_4]$ ferredoxins, and we use

the same geometry found in that paper. The cluster, depicted in Fig. 2, has a cubane-type Fe_4S_4 unit with a -SCH_3 group attached to each Fe atom. These groups are substitutes for the ferredoxin cysteine residues that link the Fe atoms to the protein.

The cluster's cubane unit is distorted. A perfect cube would have the Fe atoms (and the S atoms) in a tetrahedral arrangement with T_d symmetry. Instead, the cluster has its Fe atoms in a D_{2d} geometry, where all Fe atoms still have equivalent environments, but now with two Fe-Fe distances of 2.73 Å and 2.84 Å.

As discussed in ref. 45, the cluster's ground state is qualitatively characterized as follows. The 4 Fe atoms comprise 2 ferric (Fe^{III}; d^5; 5 unpaired electrons in high-spin configuration) and 2 ferrous (Fe^{II}; d^6; 4 unpaired electrons in high-spin configuration) sites. Fe atoms 1 and 2, hereafter jointly referred to as "frag12", consist of one high-spin (5 unpaired electrons) ferric site and one high-spin (4 unpaired electrons) ferrous site coupled to a dectet (9 unpaired electrons). Fe atoms 3 and 4, hereafter jointly referred to as "frag34", are analogously

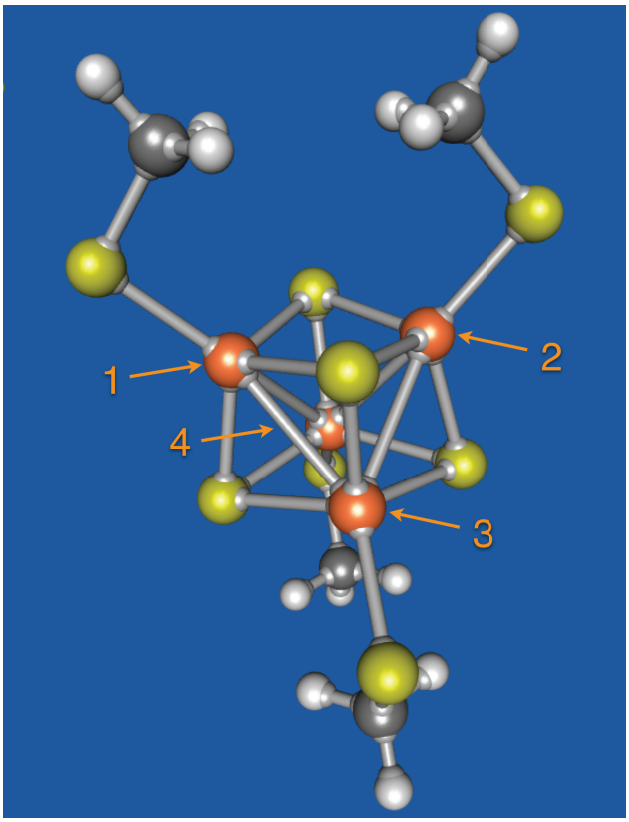

FIG. 2: View of the $Fe_4S_4(SCH_3)_4]^{2-}$ complex, with the 4 iron atoms shown in orange with labels. The geometry is taken from ref. 45.

coupled, and the two dectet fragments, one centered on frag12 and the other centered on frag34, are coupled to an overall singlet. Crudely, this state is within the UHF scope (though it will break symmetry): we can assign α spins to 9 singly occupied orbitals on frag12, and do likewise with β spins on frag34. Similarly, CCVB should be appropriate for this state, and so we would not expect the latter to entail significant 3-pair amplitudes. This will be confirmed below. As stated in the Introduction, 3-pair correlation must be essential to some states of this complex, and we will now direct this inquiry to the low-lying excited singlet states.

The ground state indicates that the ferric and ferrous sites are preferentially high spin. Taking a step back from the ground state and looking at this complex more broadly, there are several schemes for spin coupling these 4 sites to an overall singlet. We will focus here on configurations that are couplings of a well-defined spin state on frag12 with a well-defined spin state on frag34 as summarized in Figure 3. In other words, Fe atoms 1 and 2 can be coupled to any of $s = \frac{1}{2}, \frac{3}{2}, \frac{5}{2}, \frac{7}{2}, \frac{9}{2}$, and each of these can be coupled with the same type of spin coupling for Fe atoms 3 and 4 to form an overall singlet. We will denote these couplings by $\left[\frac{i}{2}\right]$–$\left[\frac{i}{2}\right]$, where the first and second numbers refer to the local spin values of frag12 and frag34, respectively, and i is one of 1,3,5,7,9. Because the ground state is antiferromagnetic, these 5 singlet configurations should be low-lying. Additionally, the fragment $s = \frac{3}{2}, \frac{5}{2}, \frac{7}{2}$ states are well outside the UHF scope; UHF cannot dissociate analogous states for Mn_2^+.[36] This, along with the inter-fragment spin coupling, recommends the $\left[\frac{1}{2}\right]$–$\left[\frac{1}{2}\right]$ through $\left[\frac{7}{2}\right]$–$\left[\frac{7}{2}\right]$ configurations as potential exhibitors for significant 3-pair correlation.

We briefly pause to note that there are additional low-lying singlet configurations in this complex. This comes from the indistinguishability of the sites we have labeled as ferric and ferrous, i.e. the quantum-mechanical equivalence of Fe^{2+}-Fe^{3+} and Fe^{3+}-Fe^{2+}, and also from the fact that each ferrous site, being high-spin d^6, has 5 relatively low lying local states. Nevertheless, in a heterogeneous molecular environment such as this, one state will tend to dominate each ferrous site and electronic structure methods that provide an incomplete description of electron correlation effects, such as HF and even CASSCF, will tend to break the ferric-ferrous interchangability symmetry. Therefore, we will focus on the above 5 singlet spin couplings.

We must make a distinction between these configurations and the pertinent exact low-lying singlet states. Qualitatively, we expect the latter to be linear combinations of the

former. This mixing will vanish as the complex is pulled apart into two similar fragments, one containing frag12 and the other containing frag34. But the complex is relatively far from being in such a dissociated geometry, with the interfragment Fe-Fe distance being slightly *shorter* than the intrafragment distance. The following considerations will allow us to move forward. The ground state is dominated by the $\left[\frac{9}{2}\right]$–$\left[\frac{9}{2}\right]$ configuration, and so it has little if any overlap with the other 4 configurations. Therefore, the $\left[\frac{1}{2}\right]$–$\left[\frac{1}{2}\right]$ through $\left[\frac{7}{2}\right]$–$\left[\frac{7}{2}\right]$ configurations are essentially linked to excited states, these configurations qualitatively underlying the low-lying states of interest. In this paper, we are not interested in any particular excited state. We want to know if 3-pair correlation is important for the low-lying states collectively. For this basic question, we can use the $\left[\frac{i}{2}\right]$–$\left[\frac{i}{2}\right]$ configurations as surrogates for the exact states. The above discussion suggests that this question will be answered affirmatively. To test this, we will design individualized CCVB-i3 calculations corresponding to each of the $\left[\frac{i}{2}\right]$–$\left[\frac{i}{2}\right]$ configurations. For now, we will continue the abstract discussion before moving on to more concrete calculations.

In a recent paper[36], we computed a ladder of spin states with CCVB by first obtaining a CCVB solution for the lowest spin, then converting this solution's most polarized CCVB pair to high spin and using this to initiate a CCVB calculation for the next highest spin in the ladder, and so on. We will use a very similar strategy here. The idea is that we now

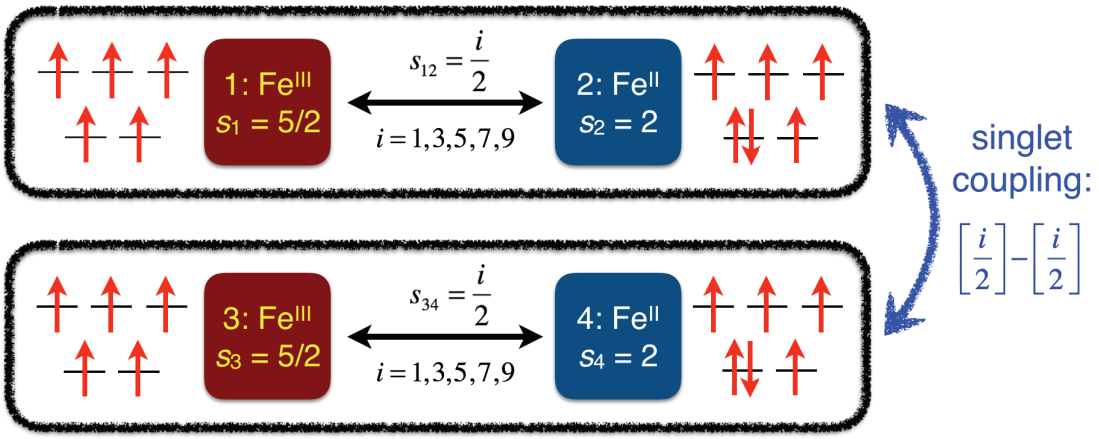

FIG. 3: Schematic showing the possible spin couplings, denoted by $\left[\frac{i}{2}\right]$, where $i = 1, 3, 5, 7, 9$, within a unit containing one high spin ferric and one high spin ferrous atom (c.f. the units denoted by frag12 and frag34 in the text), and between units, as $\left[\frac{i}{2}\right]$–$\left[\frac{i}{2}\right]$, to yield overall singlet spin. Mixed valence effects are ignored in this diagram.

effectively have two spin ladders, one on frag12 and the other on frag34. We start from the lowest spin in each ladder, i.e. with the $\left[\frac{1}{2}\right]$–$\left[\frac{1}{2}\right]$ state. A CCVB representation of a doublet on frag12 would consist of 4 CCVB pairs, each containing a localized orbital from Fe atom 1 and one from Fe atom 2, and one singly occupied orbital localized on Fe atom 1 or Fe atom 2, presuming no mixed valence effects. Because this is an antiferromagnetic interaction between Fe sites, each CCVB pair would be highly polarized, and each CCVB doubles amplitude would be large in magnitude, both the ones correlating two pairs and the ones correlating a pair and the singly-occupied orbital. This is similar to what is found in Mn_2^+.[36]

Because of the equivalence of frag12 and frag34, there is a CCVB representation of a doublet on frag34 that corresponds piece-by-piece to the one on frag12. A CCVB representation of $\left[\frac{1}{2}\right]$–$\left[\frac{1}{2}\right]$ is then obtained by joining the 4 pairs of frag12 with the 4 pairs of frag34 and putting the 2 singly occupied orbitals for the two sites into a new CCVB pair. In general, any pair with one orbital on each fragment will be referred to as "mixed fragment", and any pair with both orbitals on one fragment will be referred to as "same fragment". The 9 pairs above have just 5 unique polarization angles: one for the mixed-fragment pair and 4 for the same-fragment pairs due to the frag12-frag34 equivalence. Again, all of these pairs would be highly polarized.

For an isolated frag12, the spin-ladder guessing scheme would produce a quartet by converting the doublet's most polarized pair to high spin. This works similarly for frag34. The analogous procedure within the CCVB representation of $\left[\frac{1}{2}\right]$–$\left[\frac{1}{2}\right]$ is to look at the 4 same-fragment pair duos, select the most polarized one, and rearrange the 4 orbitals in these 2 pairs to obtain 2 new mixed-fragment pairs. This gives an initial guess for $\left[\frac{3}{2}\right]$–$\left[\frac{3}{2}\right]$. Selecting the most polarized pair duo of the remaining same-fragment pairs and rearranging the 4 orbitals into 2 new mixed-fragment pairs gives an initial guess for $\left[\frac{5}{2}\right]$–$\left[\frac{5}{2}\right]$. This may be continued for the remaining configurations. Each time we rearrange 2 same-fragment pairs to get 2 new mixed-fragment pairs, we have a choice: if we label the 4 orbitals as o1, o2, o3, o4, based on which Fe atom they are localized to, then we begin with two pairs (o1,o2),(o3,o4) and we can rearrange to get either (o1,o3),(o2,o4) or (o1,o4),(o2,o3). We chose to rearrange so as to evenly distribute the mixed-fragment pairs around the Fe_4 unit; this provides the best compatibility with the unit's D_{2d} symmetry. The resulting pairing structures are depicted in Fig. 4.

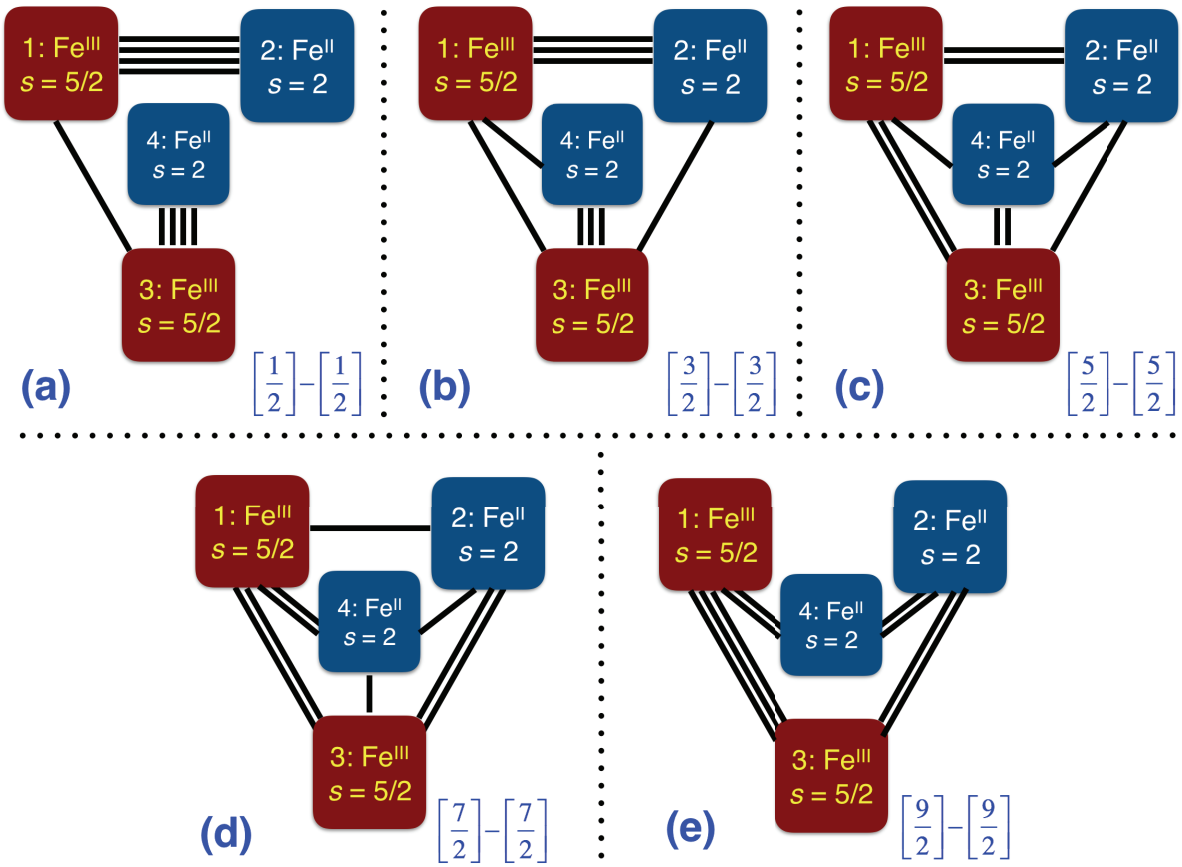

FIG. 4: Structure of the PP pairs for each singlet spin-coupling configuration. Each bond represents a (almost fully polarized) pair that is localized to the pertinent atoms.

We can now make these CCVB concepts more concrete. To calculate a CCVB representation for $[\frac{1}{2}]–[\frac{1}{2}]$, we began by obtaining a UHF solution corresponding to $[\frac{1}{2}]–[\frac{1}{2}]$. For this and all other calculations in this subsection, we used the following mixed basis set: Wachters+f[54–56] for the Fe atoms, 6-31+G*[57,58] for the S atoms, and 6-31G[59] for the C and H atoms. This was chosen for a good compromise between accuracy and speed. The basis is triple-zeta plus polarization for Fe, double-zeta plus polarization for S, along with diffuse orbitals on these atoms, and thus it should be sufficiently accurate for our purposes. For the CCVB-type calculations, we used the resolution of the identity (RI) approximation.[60–62] For this, we used a mixed auxiliary basis set as follows (where we state the corresponding correlation consistent bases): cc-pVTZ for Fe (the i orbitals were discarded),[63] aug-cc-pVDZ for S,[64,65] and cc-pVDZ for C and H.[64,65] Parameters for some of these bases were obtained from the Basis Set Exchange.[66,67]

This UHF solution has Mulliken spin values of 4.5, -3.9, -4.5, 3.9 for Fe atoms 1 through

4. Thus this solution contains high-spin ferric and ferrous sites such that there are local s_z values of $\frac{1}{2}$ and $-\frac{1}{2}$ on frag12 and frag34, respectively. Next, we used the UHF corresponding orbitals of this solution as an initial guess for a CCVB calculation, as described in our previous publications.[33,35] This produces CCVB orbitals that are delocalized between frag12 and frag34. This delocalization, although not incorrect, is at odds with the above localization-based blueprint, thus making it difficult to obtain CCVB results for the other spin-coupling configurations. To get around this, we started a PP calculation from the UHF corresponding orbitals. The resulting PP orbitals, as is almost always the case, are well localized; here, each (valence-bond form) PP orbital is localized to an Fe atom. This PP solution happened to have 3 mixed-fragment pairs, so we rearranged two of the pairs to compensate and then restarted the PP calculation. The result was in line with our blueprint, i.e. with Fig. 4 (a). We therefore decided to use PP orbitals for all CCVB calculations below, i.e. optimize orbitals with PP and then simply perform a CCVB amplitude calculation. The PP calculations for the other spin-coupling configurations were initiated with the above spin-ladder guessing scheme. We verified that in each case, the PP optimized orbitals have the desired locality and pairing arrangements, as in Fig. 4. In every case, all pairs were nearly fully polarized.

We then calculated CCVB, PP+i2, and CCVB+i3 amplitude solutions at the fixed PP orbitals for the various states. The PP+i2 amplitudes were used to initiate the CCVB and CCVB+i3 calculations. In the $\left[\frac{1}{2}\right]$–$\left[\frac{1}{2}\right]$ and $\left[\frac{9}{2}\right]$–$\left[\frac{9}{2}\right]$ cases, the CCVB+i3 solutions found this way had higher energies than those of CCVB. Restarting those CCVB+i3 calculations with the CCVB amplitudes resulted in new solutions with energies below the CCVB ones. For the other states, the CCVB+i3 energies were all well below those of CCVB. For a consistency check, we re-did those CCVB calculations starting from these CCVB+i3 amplitudes, and the resulting solutions were the same as originally obtained.

The energies of the above calculations are shown in Table I. The $\left[\frac{1}{2}\right]$–$\left[\frac{1}{2}\right]$ and $\left[\frac{9}{2}\right]$–$\left[\frac{9}{2}\right]$ results show little deviation between CCVB and CCVB+i3, while the differences are significant for the other 3 couplings. For the CCVB+i3 $\left[\frac{9}{2}\right]$–$\left[\frac{9}{2}\right]$ solution, all the 2-pair amplitudes are large, in the range 0.5-0.6, while the largest 3-pair amplitude has a magnitude of only 0.03. This wave function is therefore approximately equal to the spin projection of a determinantal wave function with α spins on the frag12 orbitals and β spins on the frag34 orbitals (the latter would have uniform amplitudes equal to $\frac{1}{\sqrt{3}}$ and 3-pair amplitudes equal

TABLE I: $[Fe_4S_4]$-complex energies (a.u.). CCVB, PP+i2, and CCVB+i3 calculations used fixed PP orbitals.

spin coupling	PP	CCVB	PP+i2	CCVB+i3
$\left[\frac{1}{2}\right]$–$\left[\frac{1}{2}\right]$	-8388.04970	-8388.49567	-8388.45926	-8388.49568
$\left[\frac{3}{2}\right]$–$\left[\frac{3}{2}\right]$	-8388.06809	-8388.41703	-8388.43307	-8388.47220
$\left[\frac{5}{2}\right]$–$\left[\frac{5}{2}\right]$	-8388.08013	-8388.35575	-8388.42587	-8388.46049
$\left[\frac{7}{2}\right]$–$\left[\frac{7}{2}\right]$	-8388.07980	-8388.34510	-8388.42929	-8388.46659
$\left[\frac{9}{2}\right]$–$\left[\frac{9}{2}\right]$	-8388.08259	-8388.50063	-8388.43479	-8388.50073

to 0). This is consistent with the above description of the ground state, suggesting that CCVB itself is qualitatively accurate here (within the appropriate (18,18) active space).

The magnitude of the largest 3-pair amplitude for the $\left[\frac{1}{2}\right]$–$\left[\frac{1}{2}\right]$ calculation is only 0.02. A low amount of 3-pair correlation was expected for $\left[\frac{9}{2}\right]$–$\left[\frac{9}{2}\right]$, but not for $\left[\frac{1}{2}\right]$–$\left[\frac{1}{2}\right]$. For the latter, we would expect there to be significant 3-pair amplitudes involving the mixed-fragment pair. In addition, we would expect the 2-pair amplitudes corresponding to one frag12 pair and one frag34 pair to be small, but this is not so in these calculations. Thus the CCVB and CCVB+i3 wave functions here are not purely $\left[\frac{1}{2}\right]$–$\left[\frac{1}{2}\right]$ couplings. Again, this is not very surprising given the fact that frag12 and frag34 are not distantly interacting fragments. In other words, although we have directed the calculations toward the various spin couplings by carefully choosing the pairing structure, the amplitudes need not strictly adhere to such a constraint. This issue is not of significant concern for our objective, because again we are not focused on any particular excited state. What is more important is that the $\left[\frac{1}{2}\right]$–$\left[\frac{1}{2}\right]$ through $\left[\frac{7}{2}\right]$–$\left[\frac{7}{2}\right]$ approximations have low overlaps with that for $\left[\frac{9}{2}\right]$–$\left[\frac{9}{2}\right]$. We provide supporting arguments for this in the Appendix.

The discrepancy between CCVB and CCVB+i3 for $\left[\frac{3}{2}\right]$–$\left[\frac{3}{2}\right]$ through $\left[\frac{7}{2}\right]$–$\left[\frac{7}{2}\right]$ implies that at least some of the 3-pair amplitudes for these couplings are large. This is indeed the case, with each of these couplings having several such amplitudes. An advantage of the symmetry-broken localized PP orbitals that we have used is that 3-pair amplitudes with significant magnitude may be grouped into 4 types based on the arrangements of their associated atomic pairs. Examples for each of these are shown in Fig. 5. We label these

types "triangle", "xbar", "zigzag", and "u" based on the appearance of the 3 associated pairs when the latter are represented with lines (i.e. bonds) and viewed in a 2-dimensional projection of the Fe_4 unit. The pairs for the triangle type involve 3 Fe atoms, and the pairs for the other types involve all 4 Fe atoms and comprise 2, 1, and 0 same-fragment pairs for xbar, zigzag, and u, respectively. These latter 3 amplitude types all have in common that their pair arrangements appear, in Fig. 5, like a path traversing the 4 Fe atoms. The values of the largest amplitudes of each type for the $\left[\frac{3}{2}\right]$–$\left[\frac{3}{2}\right]$, $\left[\frac{5}{2}\right]$–$\left[\frac{5}{2}\right]$, and $\left[\frac{7}{2}\right]$–$\left[\frac{7}{2}\right]$ states are given in Table II.

The 3-pair amplitude results may be summarized in the following three considerations. First, the 3-pair amplitudes that involve double or triple bonds (in the style of the above figures) are small for all 5 spin-coupling configurations. Second, the amplitude types with single bonds in path-like pairing arrangements, which involve either 3 atoms (triangle) or 4 atoms (xbar, zigzag, u), include large amplitudes for the $\left[\frac{3}{2}\right]$–$\left[\frac{3}{2}\right]$, $\left[\frac{5}{2}\right]$–$\left[\frac{5}{2}\right]$, and $\left[\frac{7}{2}\right]$–$\left[\frac{7}{2}\right]$ spin couplings, but not for the $\left[\frac{1}{2}\right]$–$\left[\frac{1}{2}\right]$ and $\left[\frac{9}{2}\right]$–$\left[\frac{9}{2}\right]$ spin couplings. Third, the remaining amplitude type, whose pair arrangements have the appearance of a tripod, with 3 bonds

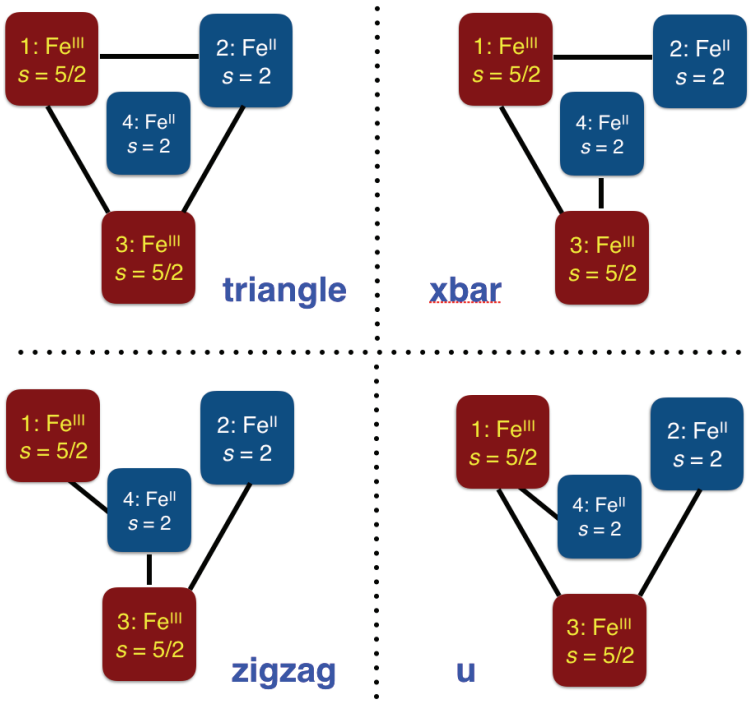

FIG. 5: Types of 3-pair amplitudes with significant magnitude. Each bond represents a pair that is localized to the pertinent atoms, c.f. Fig. 4.

TABLE II: Selected CCVB+i3 3-pair amplitudes for the $[Fe_4S_4]$ complex. Each entry is the value of the largest amplitude of the indicated type for the indicated spin-coupling configuration. The amplitude types are depicted in Fig. 5. Some of the amplitudes in this table correspond to different (but still equivalent) pair arrangements from those in the figure, e.g. the mixed-fragment pair of an xbar arrangment involving Fe atoms 1 and 4 instead of 1 and 3.

spin coupling	triangle	xbar	zigzag	u
$\left[\frac{3}{2}\right]$–$\left[\frac{3}{2}\right]$	0.456	0.439	0.060	-0.288
$\left[\frac{5}{2}\right]$–$\left[\frac{5}{2}\right]$	0.531	-0.404	0.177	-0.293
$\left[\frac{7}{2}\right]$–$\left[\frac{7}{2}\right]$	0.696	-0.512	0.528	0.143

emanating from 1 atom to each of the other 3, has small amplitudes for all 5 spin couplings.

The observation of large triangle-type amplitudes is expected given the known association of this geometrical arrangment with spin frustration. This is similar to the above O_3 example. The observation of large amplitudes of the other types (xbar, zigzag, u), is perhaps more unforseen. It is interesting that although the $\left[\frac{1}{2}\right]$–$\left[\frac{1}{2}\right]$ configuration has xbar amplitudes, and the $\left[\frac{9}{2}\right]$–$\left[\frac{9}{2}\right]$ configuration has u amplitudes, they are all small. This is due to the numerator of the rhs of eqn. 25. This is a subtle matter in this complex: as we move between spin-coupling configurations, certain amplitudes go from being significant to small, despite significant 2-pair amplitudes for the associated indices. In other words, the 2-pair amplitudes alone do not indicate the nature of the associated 3-pair amplitudes, rather the combination of amplitude signs and matrix-element values is material.

IV. CONCLUSIONS

The coupled cluster valence bond (CCVB) model is a simple theory of electron correlation that can describe some important classes of strong spin correlations, such as those associated with chemical bond breaking. CCVB yields size-consistent energies, from a spin-pure wavefunction, and CCVB can correctly separate any molecule into atoms that UHF can dissociate. The latter property reflects an underlying connection between CCVB and projected UHF: CCVB correctly describes the recoupling of pairs of electron pairs, and products of

such operators are all that arise in the PUHF wavefunction.

One limitation of CCVB arises when strong spin correlations entangle or recouple 3 electron pairs at once, as occurs in the separation of singlet molecules into fragments that cannot be properly described by UHF or PUHF (e.g. separating CO_2 into triplet C and two triplet O atoms). In this work, CCVB is extended to include the effect of 3-pair recouplings, using an independent amplitude approximation for those 3-pair couplings to define the CCVB+i3 method. A similar independent amplitude approximation could be used to treat the 2-pair recouplings, defining a simple extension, PP+i2, to the perfect pairing model that treats pair correlations without any recoupling.

The 3-pair model, CCVB+i3, is computationally as tractable as CCVB itself, while being able to treat larger classes of strong correlation problems. CCVB+i3 is size-consistent, but has no variational bound, like CCVB itself. CCVB+i3 does not resolve other limitations of CCVB, such the omission of ionic excitations, which lead to difficulties in treating systems with multiple resonance structures. PP+i2 is useful as an initial guess to the CCVB amplitudes, and has the striking feature of also being able to separate any molecule correctly into fragments (i.e. a capability beyond the CCVB model it approximates). However, as defined, PP+i2 is not always numerically stable, while CCVB+i3 appears to be as stable as the parent CCVB method.

Two example calculations are presented to explore the performance of the CCVB+i3 method, and the nature of 3-pair correlations, and when they are significant. The first example, the symmetric dissociation of singlet D_{3h} ozone, is a textbook case where UHF and PUHF cannot achieve the correct separated atom limit of 3 triplet O atoms. CCVB+i3 does achieve the correct limit, using the minimal 3-pair active space. Although the shape of the CCVB+i3 PES is qualitatively correct, it is underbound by more than 20 kcal/mol relative to the CASSCF result, which itself is underbound due to the neglect of dynamic correlation. This serves as a reminder that general application of CCVB and CCVB+i3 will require some treatment of these missing correlation effects, e.g. via a perturbation correction. Such modifications are of interest in future work.

The second example concerns the singlet states of an $[Fe_4S_4(SCH_3)_4]^{2-}$ cluster which is a model of the iron-sulfur core of $[Fe_4S_4]$ ferredoxins. The 3-pair recouplings are demonstrated to be significant in the low-lying excited singlet states, though they are not large in the ground state. These significant 3-pair recouplings include the anticipated triangular motifs

associated with spin frustration, as well as a variety of other geometric arrangements of entangled pairs. There are no cases where large 3-pair recouplings involve multiple pairs between the same two Fe atoms. It should be noted that, for this example, setting up the CCVB+i3 calculations was somewhat convoluted. It required a compatible pairing of localized orbitals, then adjustment of the orbital pairings for each excited state, and generally a significant amount of user input. Thus, at present, the application of CCVB+i3 to excited states is not usually a straightforward task. While the main application of CCVB+i3 is not excited states, finding the right orbitals and pairings can also be difficult for ground-state calculations. Nevertheless, the calculations in this paper have provided a fresh perspective on the nature of the low-lying excited states of cubane-type iron-sulfur clusters, namely that these states entail spin frustration, and on the nature of spin frustration more generally, namely that its scope is broader that what is observed in the archetypal odd-numbered rings of atoms. These results were obtained using wave functions parameterized by a very modest number of variables.

There are a number of interesting future research issues regarding CCVB+i3. The major limitation of the theory and implementation described in this work is that it is restricted to even electron molecules in singlet states. The generalization of CCVB itself to open shell systems was successfully accomplished[36], and we intend to report a corresponding generalization of CCVB+i3 in the near future[46]. Such a method will open larger classes of entangled states to study by CCVB+i3. Finally, a general disadvantage of valence-bond methods of the CCVB type (part of the price to be paid for the advantage of low-order polynomial compute cost) is lack of orbital invariance which often leads to multiple minima problems associated with orbital optimization. Solutions to this issue that do not dramatically increase the computational effort would also be very desirable.

ACKNOWLEDGEMENTS

This research was supported by the Director, Office of Science, Office of Basic Energy Sciences, of the U.S. Department of Energy under Contract No. DE-AC02-05CH11231.

---

[1] W. Kohn, A. D. Becke, and R. G. Parr, J. Phys. Chem. **100**, 12974 (1996).

[2] R. O. Jones, Rev. Mod. Phys. **87**, 897 (2015).

[3] N. Mardirossian and M. Head-Gordon, Mol. Phys. **115**, 2315 (2017).

[4] L. Goerigk, A. Hansen, C. Bauer, S. Ehrlich, A. Najibi, and S. Grimme, Phys. Chem. Chem. Phys. **19**, 32184 (2017).

[5] A. T. Bell and M. Head-Gordon, Ann. Rev. Chem. Biomol. Eng. **2**, 453 (2011).

[6] J. Sun, R. C. Remsing, Y. Zhang, Z. Sun, A. Ruzsinszky, H. Peng, Z. Yang, A. Paul, U. Waghmare, X. Wu, M. L. Klein, and J. P. Perdew, Nature Chem. **8**, 831 (2016).

[7] N. Mardirossian and M. Head-Gordon, J. Chem. Phys. **144**, 214110 (2016).

[8] A. J. Cohen, P. Mori-Sanchez, and W. T. Yang, Chem. Rev. **112**, 289 (2012).

[9] T. F. Hughes and R. A. Friesner, J. Chem. Theor. Comput. **7**, 19 (2011).

[10] M. Swart, Int. J. Quantum Chem. **113**, 2 (2013).

[11] T. Helgaker, W. Klopper, and D. Tew, Mol. Phys. **106**, 2107 (2008).

[12] R. J. Bartlett and M. Musial, Rev. Mod. Phys. **79**, 291 (2007).

[13] K. Raghavachari, G. W. Trucks, J. A. Pople, and M. Head-Gordon, Chem. Phys. Lett. **157**, 479 (1989).

[14] B. O. Roos, P. R. Taylor, and P. E. M. Siegbahn, Adv. Chem. Phys. **48**, 157 (1980).

[15] P. E. M. Siegbahn, J. Almlöf, A. Heiberg, and B. O. Roos, J. Chem. Phys. **74**, 2384 (1981).

[16] K. Ruedenberg, M. W. Schmidt, M. M. Gilbert, and S. T. Elbert, Chem. Phys. **71**, 41 (1982).

[17] D. Casanova and M. Head-Gordon, Phys. Chem. Chem. Phys. **11**, 9779 (2009).

[18] P. M. Zimmerman, F. Bell, M. Goldey, A. T. Bell, and M. Head-Gordon, J. Chem. Phys. **137**, 164110 (2012).

[19] G. Li Manni, S. D. Smart, and A. Alavi, J. Chem. Theor. Comput. **12**, 1245 (2016).

[20] J. B. Schriber and F. A. Evangelista, J. Chem. Phys. **144**, 161106 (2016).

[21] N. M. Tubman, J. Lee, T. Y. Takeshita, M. Head-Gordon, and K. B. Whaley, J. Chem. Phys. **145**, 044112 (2016).

[22] G. Gidofalvi and D. A. Mazziotti, J. Chem. Phys. **129**, 134108 (2008).

[23] J. Fosso-Tande, N. Truong-Son, G. Gidofalvi, and A. E. DePrince, III, J. Chem. Theor. Comput. **12**, 2260 (2016).

[24] D. Ghosh, J. Hachmann, T. Yanai, and G. K.-L. Chan, J. Chem. Phys. **128**, 144117 (2008).

[25] G. K. L. Chan and S. Sharma, Annu. Rev. Phys. Chem. **62**, 465 (2011).

[26] P. A. Malmqvist, A. Rendell, and B. O. Roos, J. Phys. Chem. **94**, 5477 (1990).

[27] C. D. Sherrill and H. F. Schaefer, Adv. Quantum Chem. **34**, 143 (1999).

[28] D. Ma, G. Li Manni, and L. Gagliardi, J. Chem. Phys. **135**, 044128 (2011).

[29] A. I. Krylov, C. D. Sherrill, E. F. C. Byrd, and M. Head-Gordon, J. Chem. Phys. **109**, 10669 (1998).

[30] J. A. Parkhill, K. Lawler, and M. Head-Gordon, J. Chem. Phys. **130**, 084101 (2009).

[31] J. A. Parkhill and M. Head-Gordon, J. Chem. Phys. **133**, 024103 (2010).

[32] S. Lehtola, J. Parkhill, and M. Head-Gordon, J. Chem. Phys. **145**, 134110 (2016).

[33] D. W. Small and M. Head-Gordon, J. Chem. Phys. **130**, 084103 (2009).

[34] D. W. Small and M. Head-Gordon, Phys. Chem. Chem. Phys. **13**, 19285 (2011).

[35] D. W. Small, K. V. Lawler, and M. Head-Gordon, J. Chem. Theory Comput. **10**, 2027 (2014).

[36] D. W. Small and M. Head-Gordon, J. Chem. Phys. **147**, 024107 (2017).

[37] D. L. Cooper, J. Gerratt, and M. Raimondi, Int. Rev. Phys. Chem. **7**, 59 (1988).

[38] D. L. Cooper, J. Gerratt, and M. Raimondi, Chem. Rev. **91**, 929 (1991).

[39] J. Gerratt, D. L. Cooper, P. B. Karadakov, and M. Raimondi, Chem. Soc. Rev. **26**, 87 (1997).

[40] C. A. Jimenez-Hoyos, T. M. Henderson, T. Tsuchimochi, and G. E. Scuseria, J. Chem. Phys. **136**, 164109 (2012).

[41] D. W. Small and M. Head-Gordon, J. Chem. Phys. **137**, 114103 (2012).

[42] J.-H. Lee, D. W. Small, E. Epifanovsky, and M. Head-Gordon, J. Chem. Theory Comput. **13**, 602 (2017).

[43] A. C. Hurley, J. Lennard-Jones, and J. A. Pople, Proc. Roy. Soc. A **220**, 446 (1953).

[44] W. A. Goddard and L. B. Harding, Annu. Rev. Phys. Chem. **29**, 363 (1978).

[45] S. Sharma, K. Sivalingam, F. Neese, Chan, and G. Kin-Lic, Nature Chem. **6**, 927 (2014).

[46] J.-H. Lee, D. W. Small, and M. Head-Gordon, (in preparation).

[47] R. Ahlrichs and W. Kutzelnigg, J. Chem. Phys. **48**, 1819 (1968).

[48] M. Jungen and R. Ahlrichs, Theor. Chim. Acta **17**, 339 (1970).

[49] V. Staemmler and M. Jungen, Theor. Chim. Acta **38**, 303 (1975).

[50] Y. Shao, Z. Gan, E. Epifanovsky, A. Gilbert, M. Wormit, J. Kussmann, A. Lange, A. Behn, J. Deng, X. Feng, D. Ghosh, M. Goldey, P. Horn, L. Jacobson, I. Kaliman, R. Khaliullin, T. Kus, A. Landau, J. Liu, E. Proynov, Y. Rhee, R. Richard, M. Rohrdanz, R. Steele, E. Sundstrom, H. Woodcock, P. Zimmerman, D. Zuev, B. Albrecht, E. Alguire, B. Austin, G. Beran, Y. Bernard, E. Berquist, K. Brandhorst, K. Bravaya, S. Brown, D. Casanova, C.-M. Chang,

Y. Chen, S. Chien, K. Closser, D. Crittenden, M. Diedenhofen, R. DiStasio, H. Do, A. Dutoi, R. Edgar, S. Fatehi, L. Fusti-Molnar, A. Ghysels, A. Golubeva-Zadorozhnaya, J. Gomes, M. Hanson-Heine, P. Harbach, A. Hauser, E. Hohenstein, Z. Holden, T.-C. Jagau, H. Ji, B. Kaduk, K. Khistyaev, J. Kim, J. Kim, R. King, P. Klunzinger, D. Kosenkov, T. Kowalczyk, C. Krauter, K. Lao, A. Laurent, K. Lawler, S. Levchenko, C. Lin, F. Liu, E. Livshits, R. Lochan, A. Luenser, P. Manohar, S. Manzer, S.-P. Mao, N. Mardirossian, A. Marenich, S. Maurer, N. Mayhall, E. Neuscamman, C. Oana, R. Olivares-Amaya, D. ONeill, J. Parkhill, T. Perrine, R. Peverati, A. Prociuk, D. Rehn, E. Rosta, N. Russ, S. Sharada, S. Sharma, D. Small, A. Sodt, T. Stein, D.Stck, Y.-C. Su, A. Thom, T. Tsuchimochi, V. Vanovschi, L. Vogt, O. Vydrov, T. Wang, M. Watson, J. Wenzel, A. White, C. Williams, J. Yang, S. Yeganeh, S. Yost, Z.-Q. You, I. Zhang, X. Zhang, Y. Zhao, B. Brooks, G. Chan, D. Chipman, C. Cramer, W. Goddard, M. Gordon, W. Hehre, A. Klamt, H. Schaefer, M. Schmidt, C. Sherrill, D. Truhlar, A. Warshel, X. Xu, A. Aspuru-Guzik, R. Baer, A. Bell, N. Besley, J.-D. Chai, A. Dreuw, B. Dunietz, T. Furlani, S. Gwaltney, C.-P. Hsu, Y. Jung, J. Kong, D. Lambrecht, W.-Z. Liang, C. Ochsenfeld, V. Rassolov, L. Slipchenko, J. Subotnik, T. V. Voorhis, J. Herbert, A. Krylov, P. Gill, and M. Head-Gordon, Mol. Phys. **113**, 184 (2015).

[51] M. W. Schmidt, K. K. Baldridge, J. A. Boatz, S. T. Elbert, M. S. Gordon, J. H. Jensen, S. Koseki, N. Matsunaga, K. A. Nguyen, S. J. Su, T. L. Windus, M. Dupuis, and J. A. Montgomery, J. Comput. Chem. **14**, 1347 (1993).

[52] T. H. Dunning, J. Chem. Phys. **90**, 1007 (1989).

[53] D. W. Small, E. J. Sundstrom, and M. Head-Gordon, J. Chem. Phys. **142**, 094112 (2015).

[54] A. J. H. Wachters, J. Chem. Phys. **52**, 1033 (1970).

[55] A. J. H. Wachters, IBM Tech. Rept. RJ584 (1969).

[56] C. W. Bauschlicher, Jr., S. R. Langhoff, and L. A. Barnes, J. Chem. Phys. **91**, 2399 (1989).

[57] M. M. Francl, W. J. Pietro, W. J. Hehre, J. S. Binkley, M. S. Gordon, D. J. DeFrees, and J. A. Pople, J. Chem. Phys. **77**, 3654 (1982).

[58] T. Clark, J. Chandrasekhar, G. W. Spitznagel, and P. V. R. Schleyer, J. Comp. Chem. **4**, 294 (1983).

[59] W. J. Hehre, R. Ditchfield, and J. A. Pople, J. Chem. Phys. **56**, 2257 (1972).

[60] M. Feyereisen, G. Fitzgerald, and A. Komornicki, Chem. Phys. Lett. **208**, 359 (1993).

[61] F. Weigend, M. Häser, H. Patzelt, and R. Ahlrichs, Chem. Phys. Lett. **294**, 143 (1998).

[62] B. I. Dunlap, Phys. Chem. Chem. Phys. **2**, 2113 (2000).

[63] J. G. Hill and J. A. Platts, J. Chem. Phys. **128**, 044104 (2008).

[64] F. Weigend, A. Köhn, and C. Hättig, J. Chem. Phys. **116**, 3175 (2002).

[65] C. Hattig, Phys. Chem. Chem. Phys. **7**, 59 (2005).

[66] D. Feller, J. Comp. Chem. **17**, 1571 (1996).

[67] K. L. Schuchardt, B. T. Didier, T. Elsethagen, L. Sun, V. Gurumoorthi, J. Chase, J. Li, and T. L. Windus, J. Chem. Inf. Model. **47**, 1045 (2007).

Appendix A: Excited-state characterization of CCVB+i3 results for $\left[\frac{1}{2}\right]$–$\left[\frac{1}{2}\right]$ through $\left[\frac{7}{2}\right]$–$\left[\frac{7}{2}\right]$

In this Appendix, we will provide justification for viewing the CCVB+i3 $\left[\frac{1}{2}\right]$–$\left[\frac{1}{2}\right]$ through $\left[\frac{7}{2}\right]$–$\left[\frac{7}{2}\right]$ calculations as approximations to excited singlet states. The idea is to show that the wave functions for these calculations have at most low overlaps with the $\left[\frac{9}{2}\right]$–$\left[\frac{9}{2}\right]$ CCVB wave function, which again is a qualitatively good approximation to the ground state. In fact, it is enough to show that the latter wave function has at most low overlap with the parts of the former wave functions pertinent to their amplitude equations, i.e. the reference and doubly, triply, and quadruply substituted configurations.

For this, we return to the observation that the $\left[\frac{9}{2}\right]$–$\left[\frac{9}{2}\right]$ CCVB wave function is approximately the spin projection of a product of simple dectets on each fragment. We will consider the overlap of the latter wave function with the pertinent parts of the various CCVB-i3 wave functions. To simplify this, we should use the same set of orbitals for both wave functions in a given overlap. For each of the $\left[\frac{i}{2}\right]$–$\left[\frac{i}{2}\right]$ calculations, all pairs are nearly fully polarized. So, in each case, the 18 orbitals are essentially orthonormal. For each case, we can build a spin-projected determinant from these 18 orbitals (along with the doubly occupied inactive CCVB-i3 orbitals); we assign α spin to the 9 frag12 orbitals and β spin to the remaining 9 orbitals (which are on frag34). Since the α orbitals are already essentially orthonormal, and likewise for the β orbitals, we effectively can deal with these determinants in the usual way. The resulting 5 spin-projected wave functions, which will be denoted by spdet-$\left[\frac{i}{2}\right]$, are each qualitatively the same as the $\left[\frac{9}{2}\right]$–$\left[\frac{9}{2}\right]$ CCVB wave function, so we can use them to evaluate the overlaps.

The overlap of spdet-$\left[\frac{i}{2}\right]$ with a CCVB-type wave function or CCVB configuration is the

same as the overlap of the corresponding unprojected determinant, denoted by det-$\left[\frac{i}{2}\right]$, with the CCVB-type wave function or configuration, i.e. the CCVB-type wave function, being a pure singlet, "absorbs" the projection operator. det-$\left[\frac{i}{2}\right]$ has either two α spins or two β spins in each same-fragment pair position. Thus it will not overlap with any configuration that has any singlet same-fragment pairs. Therefore det-$\left[\frac{i}{2}\right]$ doesn't overlap with the reference wave function for $\left[\frac{i}{2}\right]$–$\left[\frac{i}{2}\right]$.

The first substitution level at which there can be an overlap in this context is 8-pair, 6-pair, 4-pair, and 2-pair for the $\left[\frac{1}{2}\right]$–$\left[\frac{1}{2}\right]$ through $\left[\frac{7}{2}\right]$–$\left[\frac{7}{2}\right]$ cases, respectively. Thus the overlap between det-$\left[\frac{1}{2}\right]$ and a full CCVB-type wave function for $\left[\frac{1}{2}\right]$–$\left[\frac{1}{2}\right]$ must be quite small, and more importantly, the configurations involved in the amplitude equations for the $\left[\frac{1}{2}\right]$–$\left[\frac{1}{2}\right]$ CCVB-i3 calculation do not overlap with this determinant at all. We can therefore say that the $\left[\frac{1}{2}\right]$–$\left[\frac{1}{2}\right]$ results qualitatively correspond to an excited state, or mixture thereof. The same type of reasoning leads to the same conclusion for the $\left[\frac{3}{2}\right]$–$\left[\frac{3}{2}\right]$ results.

For the $\left[\frac{5}{2}\right]$–$\left[\frac{5}{2}\right]$ results, we argue that spdet-$\left[\frac{5}{2}\right]$, being a qualitatively accurate approximation to the ground state within the (18,18) active space, should have low overlap through $\mathbf{H}$ with the reference and 2-pair substituted configurations of the $\left[\frac{5}{2}\right]$–$\left[\frac{5}{2}\right]$ wave function, and therefore it makes an inappreciable contribution to the amplitude equations for this case. This again permits us to designate these results as excited state.

For the $\left[\frac{7}{2}\right]$–$\left[\frac{7}{2}\right]$ results, we note that the only 2-pair substituted configuration of the $\left[\frac{7}{2}\right]$–$\left[\frac{7}{2}\right]$ wave function that can overlap with spdet-$\left[\frac{7}{2}\right]$ is the one corresponding to the two remaining same-fragment pairs. The CCVB-i3 amplitude for this configuration is about -0.3, so the corresponding amplitude equation may entail some influence from the ground state. But, this is just one amplitude out of a total of 36 doubles. Furthermore, several of the largest 3-pair amplitudes for this calculation, which are the ones we are most interested in presently, are orthogonal to det-$\left[\frac{7}{2}\right]$.